Journal of
Chemical Engineering and
Materials Science

ACADEMIC
JOURNALS
expand your knowledge

ABOUT JCEMS

The **Journal of Chemical Engineering and Materials Science (JCEMS)** is published monthly (one volume per year) by Academic Journals.

Journal of Chemical Engineering and Materials Science (JCEMS) is an open access journal that provides rapid publication (monthly) of articles in all areas of the subject such as semiconductors, high-temperature alloys, Kinetic Processes in Materials, Magnetic Properties of Materials, optimization of mixed materials etc.
The Journal welcomes the submission of manuscripts that meet the general criteria of significance and scientific excellence. Papers will be published shortly after acceptance. All articles published in JCEMS are peer-reviewed.

Contact Us

Editors

Dr. R. Jayakumar
Center for Nanosciences Amrita
Institute of Medical Sciences and Research
Centre
Amrita Vishwa Vidyapeetham University
Cochin-682 026
India

Prof. Lew P Christopher
Center for Bioprocessing Research and
Development(CBRD)
South Dakota School of Mines and
Technology(SDSM&T)
501 East Saint Joseph Street
Rapid City 57701 SD
USA

Prof. Huisheng Peng
Laboratory of Advanced Materials
Department of Macromolecular Science
Fudan University Shanghai 200438
China

Prof. Layioye Ola Oyekunle
Department of Chemical Engineering
University of Lagos Akoka-Yaba
Lagos Nigeria

Dr. Srikanth Pilla
Structural Engineering and Geomechanics Program
Dept of Civil and Environmental Engineering
Stanford University
Stanford CA 94305-4020
USA.

Asst Prof. Narendra Nath Ghosh
Department of Chemistry,
Zuarinagar, Goa-403726,
India.

Dr. Rishi Kumar Singhal
Department of Physics, University of Rajasthan,
Jaipur 302055 India.

Dr. Daoyun Song
West Virginia University
Department of Chemical Engineering,
P. O Box 6102, Morgantown, WV 26506,
USA.

Journal of Chemical Engineering and Materials Science

Table of Contents: Volume 9   Number 2   September   2018

ARTICLES

Journal of Chemical Engineering and Materials Science

AJ ACADEMIC JOURNALS
expand your knowledge

Full Length Research Paper

Production of bioethanol from stems of *Sorghum saccharatum* monitoring kinetic parameters of fermentation

I. Mossi[1], E. S. Adjou[2], C. P. A. Dossa[1], G. Nonviho[1] M. M. Conforte Adda[3], B. B. Yehouenou[2] and D. C. K. Sohounhloué[1*]

[1]Molecular Interaction Research Unit (URIM), Laboratory of Study and Research in Applied Chemistry, Polytechnic School of Abomey-Calavi, University of Abomey-Calavi, Benin (LERCA/EPAC/UAC), 01 P.O.B: 2009 Cotonou, Republic of Benin.
[2]Unit of Research in Enzymatic and Food Engineering (URGEA), Laboratory of Study and Research in Applied Chemistry, Polytechnic School of Abomey-Calavi, University of Abomey-Calavi, Benin (LERCA/EPAC/UAC), 01 P.O.B: 2009 Cotonou, Republic of Benin.
[3]Unit of Research in Natural Vegetable Extracts and Aromas (UREV), Laboratory of Study and Research in Applied Chemistry, Polytechnic School of Abomey-Calavi, University of Abomey-Calavi, Benin (LERCA/EPAC/UAC), 01 P.O.B: 2009 Cotonou, Republic of Benin.

The objective of this study was to evaluate the performance of three stumps of *Saccharomyces cerevisiae* in the ethanol bioconversion of the diluted stems of sweet sorghum (*Sorghum saccharatum* L.) and to monitor the kinetic parameters of fermentation. Therefore, different initial concentrations of three stems from *S. cerevisiae* are used to ferment the juice. The juice obtained was formulated from one kilogram (1 kg) of stems of *S. saccharatum* and 0.5 L of distilled water. The monitoring of the kinetic fermentation parameters of the musts revealed that the best production yields (28.31±0.07 and 24.23±0.07 mL/kg) from bioethanol are obtained with the fermented mashes in the presence of the *Angel brand super alcohol* (3 and 5 g/L). This study showed that the stem of *S. saccharatum* L. constitutes a good fermentable biomass that could be valorized through the production of first-generation biofuel.

Key words: Sorghum, *Saccharomyces cerevisiae*, fermentation, bioethanol.

INTRODUCTION

The control of renewable energies has become today a major concern for developing countries in order to get the planet out of the multiple nuisances related to the massive use of fossil fuels. These renewable energies are a credible alternative to fossil energy (Vinson, 2016)). Their development is a huge challenge in terms of diversification and energy security (Leclerc et al., 2014).

In Africa in general, and in Benin in particular, the biofuels sector is still in its infancy due to persistent problems related to hunger, health, youth unemployment and low income. As the policy of developing countries is generally to eradicate hunger, endemic diseases and ensure the best social coverage of population, it seems inappropriate, if not impossible, to produce bioethanol in t

and low income. As the policy of developing countries is generally to eradicate hunger, endemic diseases and ensure the best social coverage of population, it seems inappropriate, if not impossible, to produce bioethanol in a country where people are dying from hunger.

Bioethanol production may be poorly perceived. In order to find solutions to the problems of hunger, livestock fodder and energy distribution, with the aim of reducing greenhouse gases, decision-makers had thought in 2012 about the species of cereals capable to provide leaves, bagasse and sugars (Ren et al., 2012). Among these renewable biomasses is the species *Sorghum saccharatum* (L) which is a plant with multiple potential uses. Sweet sorghum is considered a promising energy crop for biofuel production (Carrillo et al., 2014; Yin et al., 2013). The grains of sweet sorghum contain various high value-added molecules (tannins, anthocyanins, kafirines, aconitic acid, etc.) that are used in agribusiness (Temple et al., 2017). Because of the diverse uses of sorghum grain in human nutrition in sub-Saharan Africa, they are better appreciated (FAOSTAT, 2016; Pierre Gary, 2012). Sorghum stalks are lignocellulosic biomass in energy production through anaerobic digestion, thermometry, ethanol fuel production, composite plastics and building block manufacturing (Chantereau et al., 2013). The leaves and bagasses are used for fodder with high nutritional value in different forms (green, hay or ensilage). (Braconnier et al., 2014). Due to its plasticity and great diversity of forms, sorghum can be integrated into many growing systems in tropical and temperate zones (Damasceno et al., 2014; Vinutha et al., 2014). It is a cover plant for soil conservation and remobilization of minerals in cropping systems. Although it is also suitable for drier and less fertile environments, it remains an essential food crop for people living in the arid and semi-arid tropics (BSI, 2018; (Vinson, 2016); Temple et al., 2017; Carrillo et al., 2014). Its ability to provide many ecosystem services makes it a culture of the future (Temple et al., 2017). As a result, average sorghum production has risen (in the last five years) to 60 million tons a year worldwide. The 2015-2016 seasons had given global sorghum production of 60.16 million tons. This production reached 64.20 million tons for the 2016-2017 crop season (COMMODAFRICA, 2016). Intensification of sorghum cultivation would contribute to solving the problems of climate change, health, food insecurity and energy distribution (Visser et al., 2005). The varieties in use of sorghum fit the various food stakes, energy and environmental challenges and will enable rural populations to improve their standard of living thanks to a better valorization of agricultural production and the creation of new local commercial sectors generating jobs. Its intensive culture could help to fight against the immigration of young people. Sweet sorghum that has the potential to provide seeds, leaves, stalks and sugars could better increase household income by keeping rural people in villages and rural areas. Sweet sorghum could generate investment and compete with cereals in the market (Chantereau et al., 2013; Damasceno et al., 2014; Vinutha et al., 2014; Temple et al., 2017). With more than 23% of world sorghum production, Africa could lead new and effective policies by contributing to development goals by 2025 in renewable energy production (COMMODAFRICA, 2016). In the development perspective, it is good to consider the production of bioethanol from this lignocellulosic sweet biomass which is grown in small quantities for its grains. It is in this line of thought that the choice of sweet sorghum (*S. saccharatum* L.) took place. Thus, the objective of this work is to value the species.

MATERIALS AND METHODS

The stem of sweet sorghum (*S. saccharatum* L.) used as plant material in the framework of this study was collected in Ségbana in the Department of Alibori (North Benin) and had been directly transported fresh to the laboratory where it had been kept at -10°C in the freezer.

Three yeast strains of *Saccharomyces cerevisiae*, mainly industrial, from the Chinese company "Angel Yeast Co., Ltd" and marketed were used in alcoholic fermentation. It includes:

i) *Angel brand Thermal-tolerant alcohol*
ii) *Angel brand super alcohol*
iii) *Angel super alcohol*.

Experimental procedure

Raw material preparation

One kilogram of stems of *S. saccharatum* had been chopped, crushed into fine particles and pressed with a mechanical press fitted with a filter in the presence of 0.5 L of distilled water. The resulting juice was sterilized at 121°C for 15 minutes (Sidney, 1984).

Preparation of yeast suspensions

The dry and active yeast strains were revived at 37±1°C in peptone water for 30 min. The three revived *S. cerevisiae* strains were used as juice ferments for sweet sorghum stems.

Fermentation

The sterilized juice, cooled with *S. saccharatum* and distributed in the fermenters, was inoculated with *S. cerevisiae* strains at different concentrations (from 1 to 5 g/L). The juice wort consisting of juice without ferment was used to evaluate the incidence of the yeasts used. The alcoholic fermentation was run in batch mode for seven (7) days at room temperature (25°C).

Monitoring of fermentation parameters

Parameters such as degree brix, relative density and pH of the musts were followed from the beginning to the end of the alcoholic fermentation:

i) The total soluble content (Brix, expressed in °Bx) of the different samples was determined by direct measurement using a Palm Abbe 201 MISCO digital portable refractometer.

ii) The pH of the juice is determined using an OHAUS ST10 digital pH-meter.

iii) The relative density at 20°C of the juices was determined according to a standard method of the Association of Official Analytical Chemists (2003) and described by Novidzro (2013).

Distillation of the must

At the end of the fermentation, the extraction of the ethanol was carried out by distillation of the musts using a QUICKFIT/FC3/13 column of vigreux distiller of 85 cm in length and 4.45 cm in diameter. During the distillation, the temperature was maintained at 79°C at the head of the vigreux column until the alcohol from the must of the heating flask was exhausted (Sidney, 1984; Novidzro et al., 2013).

Attenuation limit

This gives an estimate of the level of sugars consumed or likely to be converted into alcohol during fermentation (Novidzro, 2013).

$$Al = \frac{Brix\ iniatial - brix\ final}{Brix\ initial} \times 100 \qquad (1)$$

Determination of bioethanol yield of production

The average yield of bioethanol production of a sweet sorghum must is determined from its alcoholic strength by volume (TAV), its volume and the mass of stems used as plant material. He had given the amount of alcohol obtained as a function of the mass of sweet sorghum stems used. It is expressed by the formula:

$$R_m = \frac{V_0 V_d T_{AV}}{100 MV} \qquad (2)$$

M: Mass of stems of sweet sorghum entered in the formulation of the juice (kg)

R_m: Average yield of production

T_{AV}: Alcoholic volume title or alcoholic degree (% v/v)

V: Volume of fermented juice (mL)

V_0: Volume of distilled water used in juice formulation (mL)

V_d: Volume of distillate obtained (mL).

Statistical analyzes

The tests had been repeated three times and the data had been processed using the Microsoft Excel 2010 software. The statistical analysis of the data and the comparison of the independent averages were made at the 5% threshold by SPSS 16.0.

RESULTS AND DISCUSSION

Fermentation time

Table 1 presented the average fermentation time of the musts of stems of *S. saccharatum* (L). In the presence of *Angel brand super alcohol* and *Angel super alcohol,* the average fermentation time of musts was 48±1 h. The fermented mash containing *Thermal-tolerant alcohol* had

72±2 h. Compared to the must wort, the must sown *to Angel brand super alcohol* (and *Super Angel yeast*) then *Thermal-tolerant alcohol*, respectively had their fermentation time reduced by 72 and 48 h.

The average fermentation time of juice from pretreatment of sweet sorghum stalks is 48 h (Chen, 2012; Matsakas and Christakopoulos, 2013a;Gubicza et al., 2016). At very high density with or without urea supplement and then in the presence of *S. cerevisiae* KL17, according to Appiah-Nkansah et al. (2018), the fermentation time of flour and sweet sorghum juice is 72 h. When a sweetened biomass juice is enriched with urea, phosphorus, etc., as nutrients for yeasts, its fermentation time can be reduced. The average duration of a good fermentation of the juice of a lignocellulosic biomass in the presence of *S. cerevisiae* as ferment is between 48 and 72 h (Soro et al., 2012; Gbohaïda et al., 2015). Our results are in agreement with those of the authors despite different methods used during our study. This work has shown that the fermentation time of a sweet sorghum stem juice is between 48 and 72 h (Table 1).

pH of the must

Figure 1 showed evolution of the pH of the musts of *S. saccharatum* from the beginning to the end of the alcoholic fermentation. Overall, the curves showed the same pace. Two major phases are observed in the pH variation.

A decay phase was observed, which lasted 48 h, during which the pH of all the musts usually dropped. The mashes with *Thermal-tolerant alcohol* (Figure 1A) and *Angel super alcohol* (Figure 1C) which initially had their pH equal 4 had dropped to 3.65 in 48 h of fermentation. After 48 h also, the pH of the musts containing *Angel brand super alcohol* was 3.6. During this period, the juice must have a pH of 3.6. Compared to the control must, this decay phase showed that the acidification of the fermentation medium was not linked to the yeasts used but rather to the nature of the juice of sweet sorghum stems.

A constant linearization phase is observed in the vicinity of the pH equal to 3.5. The linear phase is between the 2nd and the 7th day of the alcoholic fermentation. In the constant linearization phase, the pH of the musts did not significantly vary, except for the pH of the must with *Angel super alcohol* of initial concentrations 1, 3 and 4 g/L of Figure 1C. In particular, the rise in pH is between the 4th and 7th day of fermentation of must containing *Angel super alcohol* at initial concentrations 1, 3 and 4 g/L.

In the works of Gubicza et al. (2016) on the pretreated stems of sweet sorghum, the pH of the musts is maintained at 6.3 during the fermentation of the juice for a better yield and at 37°C. The increase in acidity could

Table 1. Fermentation time from stem of *Sorghum saccharatum* (in hours).

Must	Initial yeast concentration (g/L)					
	0	1	2	3	4	5
Thermal-tolerant alcohol	120±3[a]	72±2[a]	72±2[a]	72±2[a]	72±2[a]	72±2[a]
Angel brand super alcohol	120±3[a]	48±1[b]	48±1[b]	48±1[b]	48±1[b]	48±1[b]
Angel super alcohol	120±3[a]	48±1[b]	48±1[b]	48±1[b]	48±1[b]	48±1[b]

Values with the same letter in the same column are not significantly different (p <5%) according to ANOVA and Tukey multiple comparison tests.
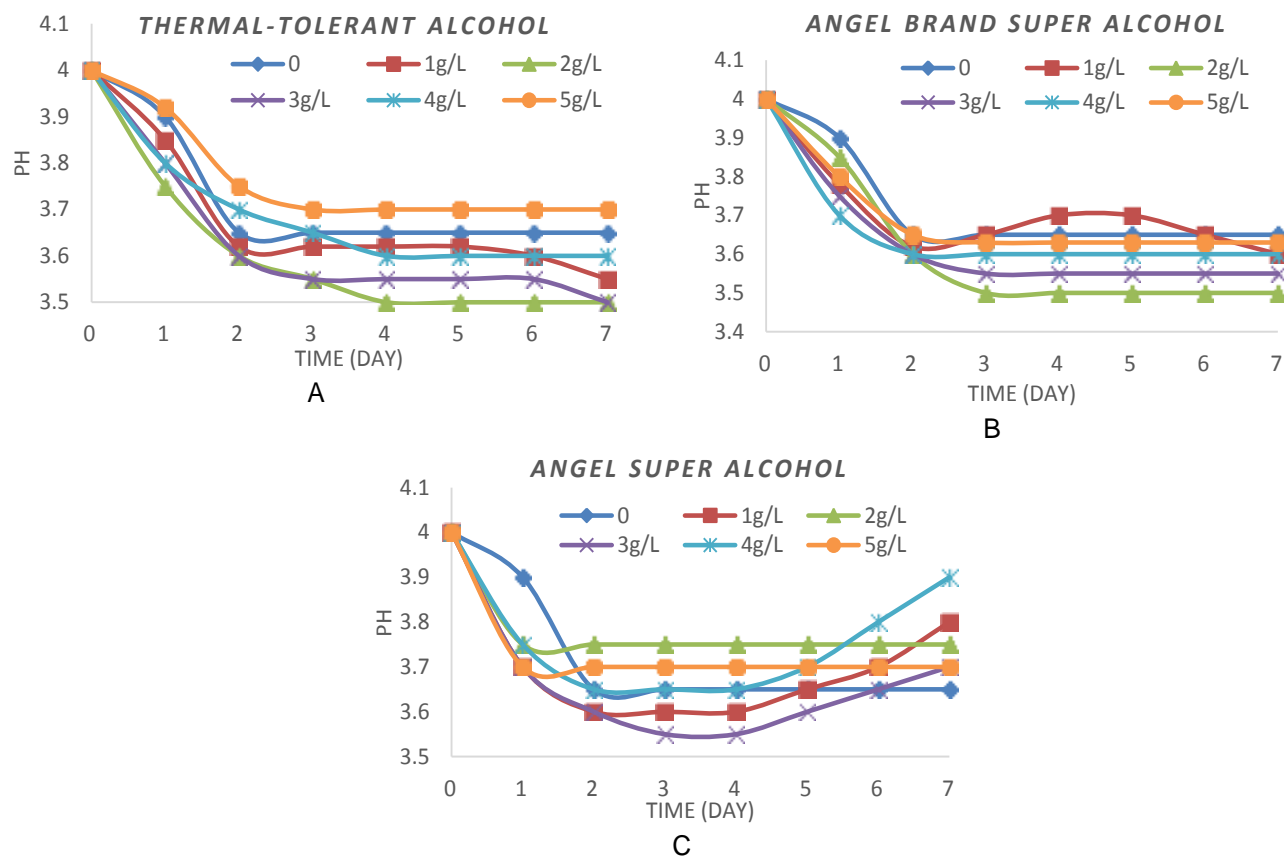
Figure 1. Variation of the pH of the different musts of *Sorghum saccharatum* during the alcoholic fermentation in the presence of (A) *Thermal-tolerant alcohol* (B) *Angel brand super alcohol* and (C) *Angel super alcohol* of *Saccharomyces cerevisiae.*

be due to the production of carbon dioxide or acidic compounds by yeasts during fermentation. The carbon dioxide (CO_2) can be dissolved in the liquid medium in the form of carbonic acid (H_2CO_3), which is dissociated into bicarbonate ions (HCO_3^-), carbonates (CO_3^{2-}) and hydrogen (H^+) (Burgot, 2011; Gbohaïda et al., 2016).

Density

The weight loss was observed (Figure 2) in the musts of *S. saccharatum* in the presence of yeast strains used at different initial concentrations. Figure 2 showed the variation of the relative density of musts during fermentation. Generally, the initial density (1.05) had dropped to 0.98. This lower density obtained after 7 days of fermentation was derived from juices containing *S. cerevisiae* at concentrations 3, 4 and 5 g/L.

Two phases were observed in the variation of the relative density. The phase of sudden loss of juice weight was observed in the first 3 days of fermentation. There had been a rapid drop in the mass of all musts. During this phase, the initial relative density of 1.05 musts decreased to 1.01. It was marked by a decrease in the

Figure 2. Variation of the density of the different musts of *Sorghum saccharatum* during the alcoholic fermentation in the presence of (A) *Thermal-tolerant alcohol* (B) *Angel brand super alcohol* and (C) *Angel super alcohol* of *Saccharomyces cerevisiae.*
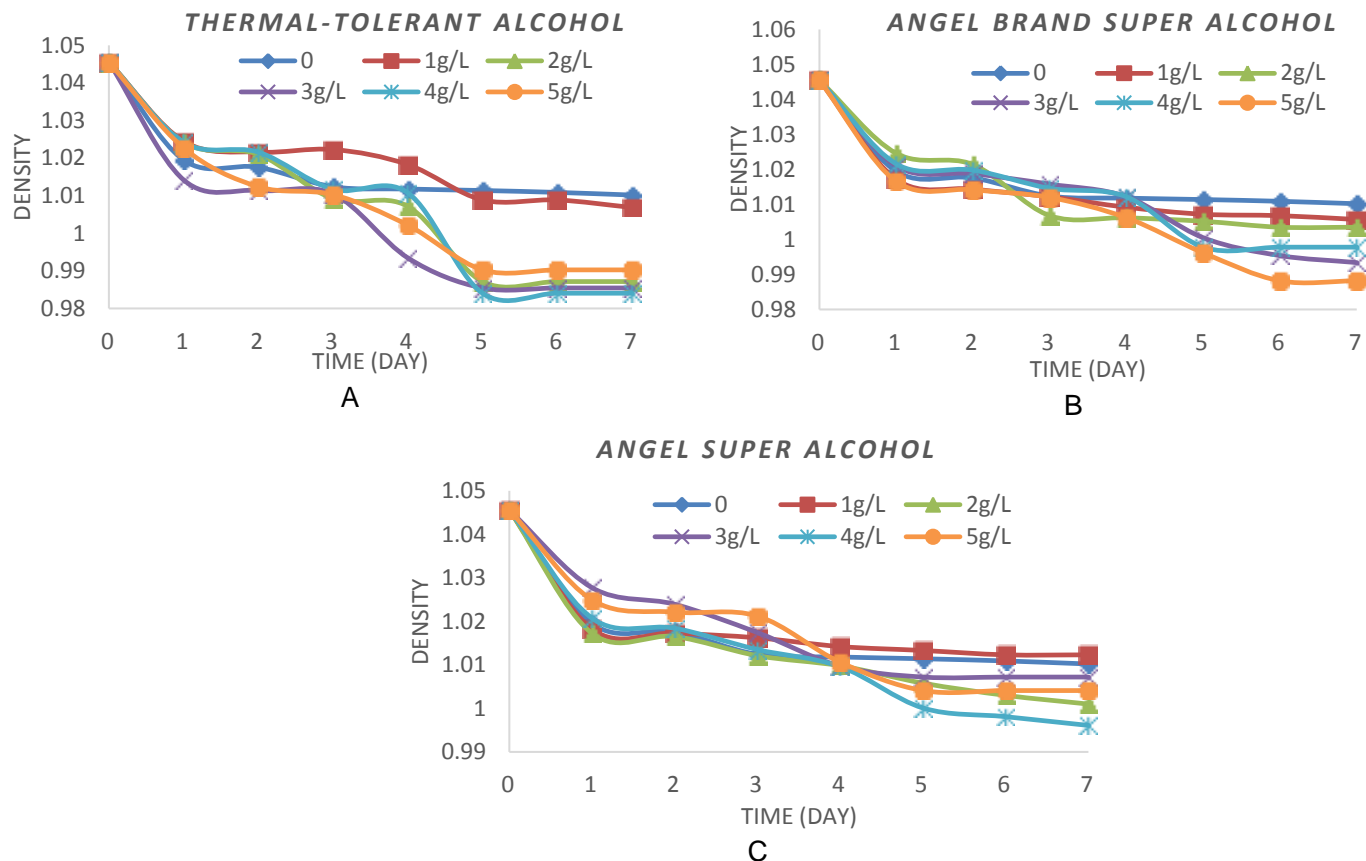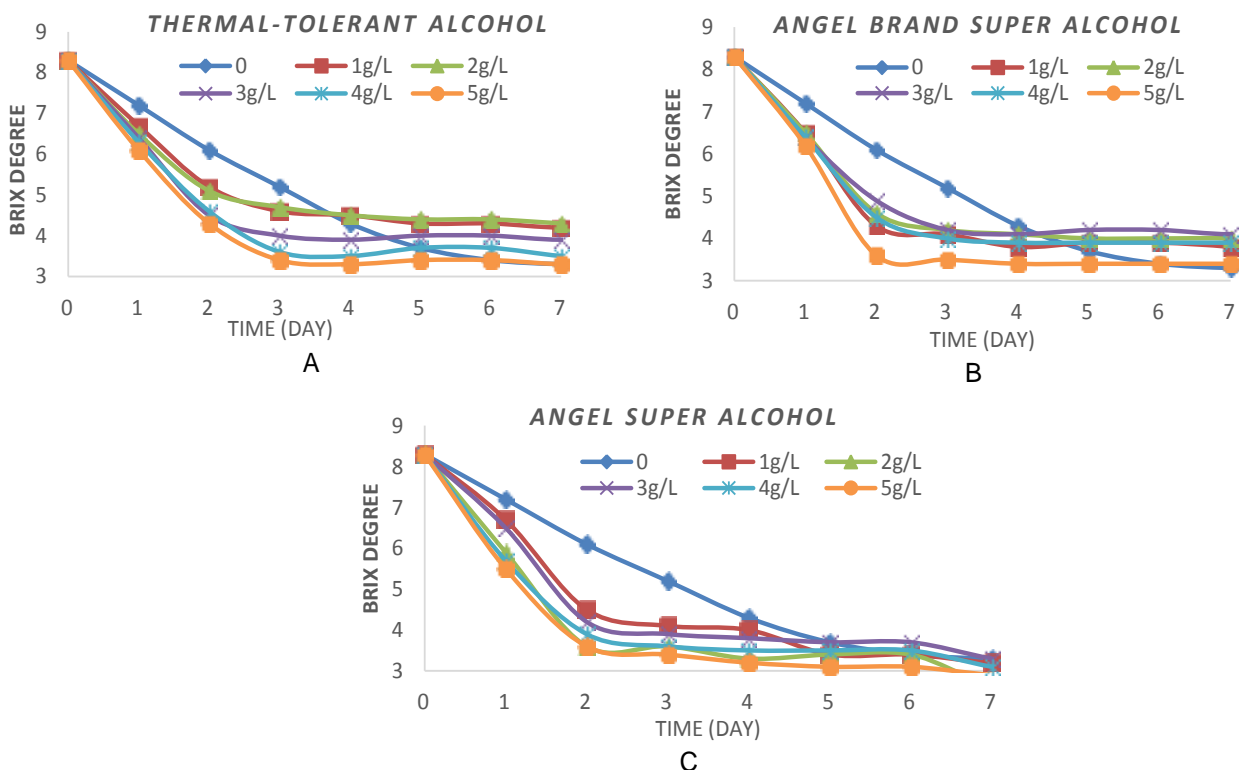
density of musts. The slowing phase was observed between the 2nd and the 7th day of fermentation. The slower weight loss of the samples started from the 1.01 density to 0.98. This phase was considered as the kinetic relaxation time of alcoholic fermentation. The work of Soro (2012), Novidzro et al. (2013) and from Gbohaïda et al. (2015) showed that the drop in the relative density of a must is closely related to the decrease in the level of soluble matter in the fermentation medium. This connection evoked by these authors was obtained in our results between Figures 2 and 3. All this showed that the loss of weight of all musts could mark the end of alcoholic fermentation.

Figure 3 provides information on the evolution of the brix degree of musts. This evolution was in agreement with the observations made in Figure 2. In 48 h of fermentation, a rapid decrease (by more than 60%) was observed in the brix level of the stem strains *Angel brand super alcohol* and *Angel super alcohol* (Figures 2B and 2C). This decrease is greater for all the concentrations of strains used. This taught us about the depletion of the total soluble solids contained in the fermentation medium. Figures 3B and 3C showed that the highest consumption of sugars by *Angel brand super alcohol* and *Angel super*

alcohol strains lasted only 48 h. Stopping the consumption of sugars marked the end of the alcoholic fermentation. The *Thermal-tolerant alcohol* must and the control respectively revealed their sugar consumption time which was 72 and 120 h (Figure 3A).

Brix degree of the must

Figure 3 presented information on the evolution of the Brix degree of the musts. This evolution was in agreement with the observations made in Figure 2. In 48 h of fermentation, a rapid decrease (by more than 60%) was observed in the brix level of the stem strains *Angel brand super alcohol* and *Angel super alcohol* (Figures 2B and 2C). This decrease is greater for all the concentrations of strains used. This taught us about the depletion of the total soluble solids contained in the fermentation medium. Figures 3B and 3C showed that the highest consumption of sugars by *Angel brand super alcohol* and *Angel super alcohol* strains lasted only 48 h. Stopping the consumption of sugars marked the end of the alcoholic fermentation. The *Thermal-tolerant alcohol* must and the control respectively revealed their sugar

Figure 3. Variation of the brix degree of the different musts of *Sorghum saccharatum* during the alcoholic fermentation in the presence of (A) *Thermal-tolerant alcohol* (B) *Angel brand super alcohol* and (C) *Angel super alcohol* of *Saccharomyces cerevisiae.*

Table 2. Attenuation limit (%).

Must	Initial yeast concentration (g/L)					
	0	1	2	3	4	5
Thermal-tolerant alcohol	60.2±0.4[a]	50.4±0.7[a]	50.6±0.4[c]	53.1±0.2[a]	59.1±0.3[a]	60.2±0.4[a]
Angel brand super alcohol	60.2±0.4[a]	56.6±0.2[b]	53.1±0.3[b]	53.1±0.4[a]	53.1±0.3[b]	59.1±0.4[a]
Angel super alcohol	60.2±0.4[a]	61.4±0.5[c]	65.1±0.4[c]	65.9±0.5[b]	66.2±0.6[c]	66.2±0.5[b]

Values with the same letter in the same column are not significantly different ($p < 5\%$) according to ANOVA and Tukey multiple comparison tests.

consumption time which was 72 and 120 h (Figure 3A).

Attenuation limit

Table 2 showed the limiting attenuation of all fermented musts. The musts containing the *Angel super alcohol* strain have a higher sugar consumption rate. Their consumption rate is between 61.2 and 66.2%. In the presence of *Angel brand super alcohol*, the musts have a rate of attenuation between 53.1 and 59.1%. The rate of limit attenuation of musts to *Angel super alcohol* and musts to *Thermal-tolerant alcohol* increases with the increase of their initial concentrations. Generally, the yeast sugar consumption rate is between 50.4 and 66.2%. These levels reveal the consumption capacity of

yeast sugars used in this study.

In the case of the alcoholic fermentation of the juice (extracted at a ratio of 1.5 L of distilled water per 1 kg of *S. saccharatum* stems), enriched with 2 g/L urea or not, in the presence of *Saccharomyces carlsbergensis* at different initial concentrations (0, 1, 2 and 3 g/L), the rate of the attenuation limit is between 72.1 and 74.4% (Mossi et al., 2017). These results may be at odds because of the different initial rates of soluble materials, yeasts used, and urea enrichment of the juice.

Average production of ethanol

Table 3 gives the average values of ethanol obtained from fermented musts of *S. saccharatum* in the presence

Table 3. Average production of ethanol (in mL/kg of stem of the *Sorghum saccharatum*).

Musts	Initial yeast concentrations					
	0	1 g/L	2 g/L	3 g/L	4 g/L	5 g/L
Thermal-tolerant alcohol	5.64±0.06[a]	12.87±0.06[a]	14.65±0.08[a]	14.60±0.08[a]	19.55±0.07[a]	12.14±0.06[a]
Angel brand super alcohol	5.64±0.06[a]	9.53±0.07[b]	18.71±0.09[b]	28.31±0.07[b]	13.97±0.07[b]	24.23±0.07[b]
Angel super alcohol	5.64±0.06[a]	13.00±0.07[c]	8.83±0.07[c]	10.21±0.09[c]	8.85±0.05[c]	7.55±0.05[c]

Values with the same letter in the same column are not significantly different (p <5%) according to ANOVA and Tukey multiple comparison tests

of *S. cerevisiae* yeasts. The most important production is obtained with the yeast *Angel brand super alcohol* and is 28.31±0.14 mL.kg^{-1} with the must of concentration 3 g.L^{-1}. 5.64 mL.kg^{-1} was collected by spontaneous fermentation of the musts of *Sorghum*. Against all odds, the production of alcohol from yeast *Angel super alcohol* has generally remained lower than that of *Thermal-tolerant alcohol* and *Angel brand super alcohol*. This could be explained by more complex biological processes not studied in this work.

The sweet sorghum bagasse pretreated with steam explosion in the presence of 7.5 FPU/g of cellulase solids gives a theoretical ethanol yield of 29.4 mL/kg after fermentation (Shen et al., 2012). Wang et al. (2013) found an ethanol yield of 49.43 mL/kg from the bagasse (10% solid) of sweet sorghum pretreated with sulfuric acid (H_2SO_4) with an enzymatic load of 29 FP/g. Kim et al. (2014), in their work report the highest concentration of ethanol (96.9 g/L) in the presence of wild-type yeast strain used (*S. cerevisiae* KL17) that is able to consume both glucose and galactose. According to Yu et al. (2014), when the work is carried out under the optimal conditions of simultaneous saccharification and co-fermentation, 49.48 mL/kg of ethanol is obtained. The result of the work of Appiah-Nkansah et al. (2018) gives 20.25% (v/v) in the production of ethanol from flour and very high density sweet sorghum juice with or without supplementation of urea by simultaneous saccharification. This productivity can reach 96% (fermentative efficiency) when the dissolved solids are at least 33% (w/v). (Matsakas and Christakopoulos, 2013b).

The research results are sometimes in agreement with those of the aforementioned authors because of the different methods of formulation and fermentation of the juice, the physicochemical composition of the plant material and the yeasts used. Some authors had pre-treated their plant material before the alcoholic fermentation by steam explosion, enzymatic hydrolysis, while others had simultaneously pretreated their material with acid and enzymatic hydrolysis.

Conclusion

The results of the present study reveal on the one hand,

the importance of *S. cerevisiae* strains in the alcoholic fermentation of *S. saccharatum* (L) stems. This work shows the fermentable bioethanol potential of sweet sorghum. The monitoring of the parameters made it possible to evaluate the pH, density, brix degree, limit attenuation and bioethanol production of the musts. It appears from this work that the *Angel brand super alcohol*, in concentrations (3 to 5 g/L) in the musts, gives better ethanol production. The intensive production of *S. saccharatum* could be a credible strategy in the fight against hunger, animal fodder and bioethanol production (FAOSTAT, 2015; Leclerc et al., 2014). In general, these results have made it possible to note that sweet sorghum could be promising. It could serve the people and allow attention to be paid to the intensive cultivation of sweet sorghum in order to provide solutions for human food, cattle fodder and bioethanol production.

CONFLICT OF INTERESTS

The authors have not declared any conflicts of interest.

REFERENCES

Association of Official Analytical Chemists (2003). Methods of Analysis Washington, 18th Edition.

Appiah-Nkansah NB, Zhang K, Rooney W, Wang D (2018). Ethanol production from mixtures of sweet sorghum juice and sorghum starch using very high gravity fermentation with urea supplementation. Industrial Crops and Products 111:247-253.

Braconnier S, Amaducci S, Basavaraj G, Borges Damasceno C, Clément-Vidal A, Fracasso A, et al. (2014). Sweet sorghum as an alternative energy crop: results from SWEETFUEL project. 22nd European Biomass Conference & Exhibition, Hamburg, 23–26 June 2014. ISBN 978-88-89407-523.

BSI (2018). BSI-Economics Renewable energies in Latin America, http://www.bsi-economics.org/693-amlat-energies-renouvelables. Accessed 26 Feb 2018.

Burgot BJL (2011). Analytical Chemistry and Ionic Balances, 2nd Edition. 11, rue *Lavoisier*. F75008 Paris. ISBN : 978-2-7430-1360-8.

Carrillo MA, Staggenborg SA, Pineda JA (2014). Washing sorghum biomass with water to improve its quality for combustion. Fuel 116:427-431.

Chantereau J, Cruz JF, Ratnadass A, Trouche G (2013). Le sorgho. Versailles: Éditions Quae, CTA, Presses Agronomiques de Gembloux 245 p.

Chen C, Boldor D, Aita G, Walker M (2012). Ethanol production from sorghum by a microwave assisted dilute ammonia pretreatment.

Bioresource technology 110:190-197.

COMMODAFRICA (2016). La production de sorgho en Afrique progresserait de 23% en 2016/17. USDA, World Agricultural Production. http://www.commodafrica.com/14-11-2016-la-production-de-sorgho-en-afrique-progresserait-de-23-en-201617

Damasceno R, Schaffert E, Dweikat I (2014). Mining genetic diversity of sorghum as a bioenergy feedstock. In: McCann MC, Marcos SB, Nicholas C. Carpita, eds. Plants and Bioenergy. Advances in Plant Biology 4:81-102.

FAOSTAT (2016). The state of food insecurity in the world (Meeting the 2015 international hunger targets: taking stock of uneven progress) (Food and Agriculture Organization) Rome. http://www.fao.org/3/a-i4646e.pdf?

Gbohaïda V, Mossi I, Adjou ES, Agbangnan DCP, Wotto V, Avlessi A, Sohounhloué DCK (2016). Évaluation du pouvoir fermentaire de Saccharomyces cerevisiae et de S. carlsbergensis dans la production de bioéthanol à partir du jus de la pomme cajou. Journal of Applied Biosciences 101:9643-9652.

Gbohaïda V, Mossi I, Adjou ES, Agbangnan DCP, Yêhouènou BB, Sohounhloué DCK (2015). Morphological and Physicochemical Characterizations of Cashew Apples from Benin for their use as Raw Material in Bioethanol Production. International Journal of Pharmaceutics 35(2):7-11.

Gubicza K, Nieves UI, William JS, Barta Z, Shanmugam KT, Ingram LO (2016). Techno-economic analysis of ethanol production from sugarcane bagasse using a Liquefaction plus Simultaneous Saccharification and co-Fermentation process. Bioresource Technology Journal 208:42-48.

Kim JH, Ryu J, Huh IY, Hong SK, Kang HA, Chang YK (2014). Ethanol production from galactose by a newly isolated *Saccharomyces cerevisiae* KL17. Bioprocess and Biosystems Engineering 37:1871-1878.

Leclerc E, Pressoir G, Braconnier S (2014). The promising future of sweet sorghum in Haiti. Journal Field Actions 9:1-9.

Matsakas L, Christakopoulos P (2013). Fermentation of liquefacted hydrothermally pretreated sweet sorghum bagasse to ethanol at high-solids content. Bioresource Technolog 127:202-208.

Matsakas L, Christakopoulos P (2013). Optimization of ethanol production from high dry matter liquefied dry sweet sorghum stalks. Biomass Bioenergy 5:91-98.

Mossi I, Adjou ES, Gbaguidi BA, Agbangnan PDC, Sohounhloué DCK (2017). Valorization of extracts from sorghum stems (*Sorghum saccharatum* L) by alcoholic bioconversion. International Journal of Computer Systems 5(6):1231-1234.

Novidzro KM (2013). Production of bioethanol by alcoholic fermentation of fruit juices of: *Balanites aegyptiaca*, *Curcubitapepo*, *Dialiumguineense* and *Opilliaamentacea*, PhD. thesis: chemistry of natural substances. University of Lomé (Togo): July 10:219.

Novidzro KM, Agbodan KA, Koumaglo KH (2013). Study of the performance of four strains of *Saccharomyces cerevisiae* during the production of ethanol from enriched sucrose musts. Journal de la Société Ouest-Africaine de Chimie 35:1-7.

Pandey A (2013). Solid-state fermentation. Biochemical Engineering Journal 13:81-84.

Pierre Gary M (2012). Evaluation de la Campagne Agricole de Printemps 2012. Rapport final campagne de septembre. Coordination Nationale de la Sécurité Alimentaire (CNSA); Haïti.

Ren LT, Liu ZX, Wei TY, Xie GH (2012). Evaluation of energy input and output of sweet sorghum grown as a bioenergy crop on coastal saline-alkali land. Energy 47:166-173.

Shen F, Hu J, Zhong Y, Michael LYL, Jack NS, Liu R (2012). Ethanol production from steam-pretreated sweet sorghum bagasse with high substrate consistency enzymatic hydrolysis. Biomass Bioenergy 41:157-164.

Sidney W (1984). Official Methods of Analysis of the Association of Official Analytical Chemists (OAC) Fourteenth (Edition). Inc. 1111 North Nineteenh: Street Suite 210, Alington, Virginia 22209 USA.

Soro D (2012). Coupling of membrane processes for the clarification and concentration of cashew apple juice: performances and impacts on the quality of the products. PhD Thesis: Process and Food Sciences, Institute of Hot Regions.

Temple L, Levesque A, Lamour A, Charles D, Braconnier S (2017). Complémentarité des filières sorgho sucré et canne à sucre en Haïti: évaluation des conditions de développement sectoriel d'une innovation. Cahiers Agricultures 26:55006

Vinson F (2016). Renewable energies in Latin America, BSI-Economics. http://www.bsi-economics.org/693-amlat-energies-renouvelables

Yu H, Guo G, Zhang X, Yan K, Xu C (2009). The effect of biological pretreatment with the selective white-rot fungus Echinodontium taxodii on enzymatic hydrolysis of softwoods and hardwoods. Bioresource technology 100(21):5170-5175.

AJ ACADEMIC JOURNALS
expand your knowledge

Journal of Chemical Engineering and Materials Science

Full Length Research Paper

Effects of artificial aging heat treatment on mechanical properties and corrosion behaviour of AA6XXX aluminium alloys

Adem Onat

Sakarya University, Vocational School of Sakarya, 54290 Sakarya – Turkey.

In this study, the effects of artificial aging heat treatment on mechanical properties and corrosion behaviour of AA6XXX alloy were investigated. The effects of artificial aging time on microstructure and mechanical properties of alloy were analysed and at the same time corrosion behaviour was determined by corrosion tests. For experimental investigations, the alloy samples prepared in appropriate sizes were heated to 540°C (±0.5°C) with heating rate 10°C/min. by electrical resistance ceramic furnace. For the solution heat treatment, samples were kept in the furnace at this temperature for 4 h. The samples taken from the furnace were firstly poured into iced water at 10°C and then subjected to artificial aging at 190°C for 2, 4, 6, 10, 12 and 24 h. Finally, the samples taken from the furnace were left to cool down in stagnant air. The results show that the mechanical properties of the material were increased with increasing aging time. Corrosion tests have shown that the corrosion resistance of the alloy depends on the artificial aging time. The best value of corrosion resistance was obtained at a temperature of 190°C at 10-h aging period.

Key words: AA6XXX aluminium alloy, artificial aging, mechanical properties, corrosion behaviour.

INTRODUCTION

Aluminium is the second most used metal in the world. Due to its high specific strength (strength/weight ratio), easy formability, high thermal conductivity, compatibility with surface treatments and resistance to corrosion, aluminium and its alloys are used in a wide range of applications from automotive, building and packaging sectors to high voltage-electricity transmission lines to construction applications (Nandy et al., 2015; Mandava et al., 2014; Wu and Liao, 2013).

6XXX series aluminium alloys, containing Mg and Si as

main alloy elements have generally good extrusion and rolling capabilities. These alloys also have good corrosion resistance, especially atmospheric environments. In addition to these favourable properties, the maintenance of the gloss of the anodized surface of the 6XXX series aluminium alloys also increases the amount of commercial use day-by-day (Panigrahi and Jayaganthan, 2010; Vargel, 2004; Yuksel, 2017). At the same time, the strength of this alloy group can be substantially increased by a two-stage heat treatment (Yuksel, 2017; Mohamed
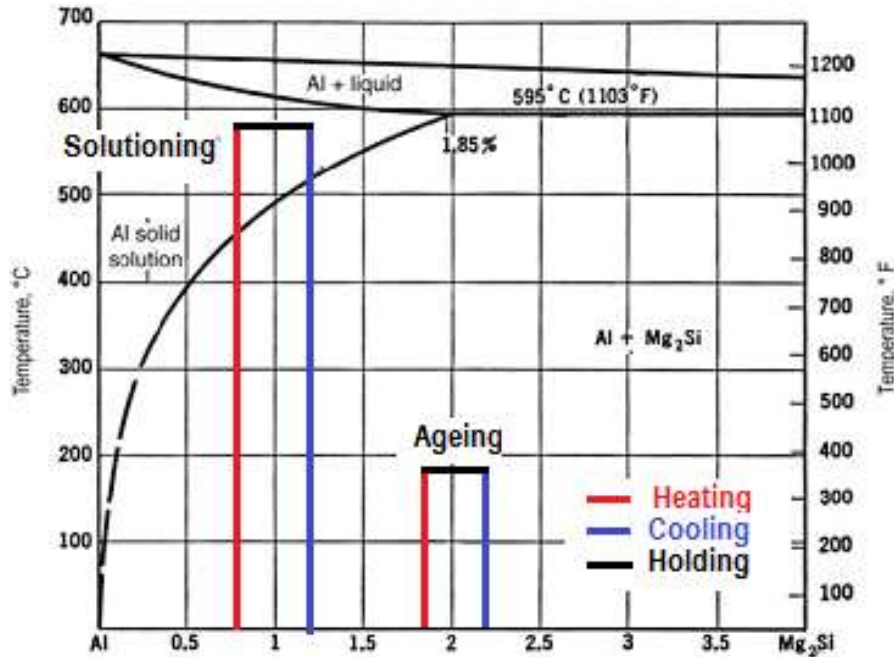
Figure 1. The schematics of precipitation heat treatment on Al-Mg$_2$Si phase diagram (8)

and Samuel, 2012).

This two-stage heat treatment consists in solutioning and ageing process. The solutioning process, holding the alloy in temperature below temperature of the eutectic reaction, is used to dissolve the precipitations of Mg$_2$Si, homogenize the chemical elements concentration on the cross-section of dendrites of the α phase and the change in the silicon precipitations morphology. The solutioning process is usually performed at 460-540°C for aluminium alloys of the 6XXX series (Figure 1).

The ageing process can be applied as natural aging at room temperature and the artificial aging at moderate temperatures. The ageing (soaking of the supersaturated alloy to separate strengthening phases from the super-saturated solid solution) and precipitation strengthening is obtained as a result of the phases precipitation of Mg$_2$Si, Al$_2$CuMg and Al$_2$Cu) (Pezda, 2014).

Artificial ageing (holding the alloy at a constant moderate temperature during predetermined period) results in the improvement of the mechanical properties such as tensile strength and hardness and in simultaneous worsening of plasticity. Because the growth of alloy's strength after heat treatment is very often accompanied with the reduction of the plasticity, their optimal relation should be selected depending on a given application of the alloy (Pezda, 2014).

In the aging phase, the precipitation process of the oversaturated melt takes place from the supersaturated solid solution (SSSS) during aging alloy going to be stable. According to the researchers, the precipitation sequence proceeds as follows: SSSS →GP zone →pre

β^{II} ((Al+Mg)$_5$Si$_6$) → β^{II} (Mg$_5$Si$_6$, Al$_3$MgSi$_6$) →β^{I} (Mg$_9$Si$_5$), β^{I}, U$_1$ (MgAl$_2$Si$_2$, MgAl$_4$Si$_5$), U$_2$ (Mg$_2$Al$_4$Si$_5$, MgAlSi) → β (Mg$_2$Si) (Edwards et al., 1998; Vissers et al., 2007).

The coherent metastable phase β^{I}, U$_1$ and U$_2$ coexists with β^{I}-phase transition. The formation of the equilibrium β phase (Mg$_2$Si) shows that there is significant strengthening of the alloy. With the increasing ratio of Mg:Si, the strength of the alloy is higher (Vissers et al., 2007). The maximum hardness is possible by obtaining the phase β^{II} during aging. On the other hand, the conversion of the β^{II} phase to the β phase is defined as over-aging, and the Face-Centred Cubic (FCC) crystal structure of the equilibrium phase β results in a reduction of the hardness of the alloy (Maisonnette et al., 2011; Li et al., 2013).

Depending on the temperature and duration of the applied artificial aging heat treatment, the type, size and quantity of the precipitated phase play an active role on the mechanical properties of the aluminium alloy and corrosion behaviour (Wu and Liao, 2013; Yuksel, 2017).

For practical applications, the corrosion resistance is one of the most decisive factors beside the mechanical properties. For this reason, in this study, the effects of artificial aging on the hardness and corrosion resistance of AA6XXX alloy were investigated.

EXPERIMENTAL STUDIES

The chemical analysis of commercial AA6XXX aluminium alloy used in this study and in rod form is given in Table 1.

Table 1. The chemical analysis of AA6XXX aluminium alloy (wt.%).

Mg	Si	Mn	Fe	Cu	Cr	Zn	Ti	Al
0.66	0.96	0.49	0.204	0.02	0.004	0.014	0.016	97.63
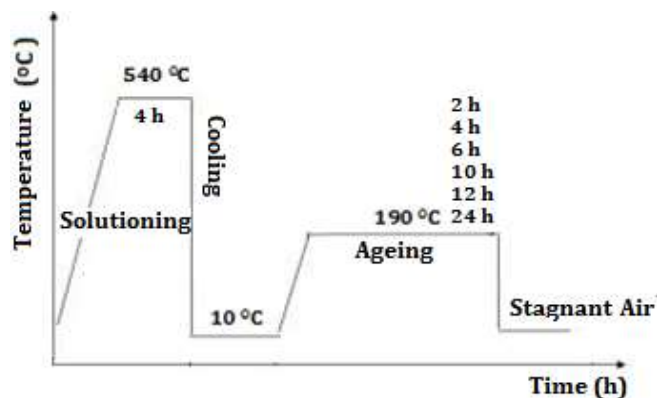
Figure 2. The schematics of heat treatment stages applied in experimental studies.

The specimens, have dimensions of 12.09 mm in diameter and 15 mm and were heated to 540 ± 0,5°C with heating rate 10°C/min in an electric resistance ceramic furnace. They were subjected to a solutioning treatment process for 4 h at this temperature. The samples taken from the furnace were first put into iced water at 10°C for 15 min and then subjected to artificial aging at 190°C for 2, 4, 6, 10, 12 and 24 h. Finally, the samples taken from the furnace were left to cool down in stagnant air. Figure 2 shows the temperature versus time (thermal) profile for the T6 heat treatment carried out on all the AA6XXX alloy samples in this study.

The heat-treated samples were prepared metallographically to examine their microstructural properties. For this purpose, the samples passed through the emery papers of 400, 600, 800, 1000 and 1200 mesh respectively were polished using 3 µm diamond paste solution and etched for about 30 s in Kellers Etch. Microstructure studies were performed using a JEOL JSM-6060LV brand SEM microscope.

The hardness measurements of the samples were carried out on a Brinell hardness tester using a 2.5 mm diameter hardened steel ball and a load of 62.5 kg. Hardness values were determined by taking the arithmetic average of at least 5 measurements for each sample.

Potentiodynamic polarization (Tafel) method was used to determine the corrosion behaviour of the samples. Three electrode techniques were used in the experiments performed in the Gamry potentiostat/galvanostat device, using saturated Ag/AgCl as the reference electrode and graphite electrodes as the auxiliary electrode. Experiments were performed at room temperature and 3.5% NaCl solution, and potentiodynamic polarization measurements were carried out at 5 mV/s for 3600 s with a voltage between -1 and +1 V. Prior to the corrosion tests, the surfaces of the specimens, 12.09 mm in diameter and 5.16 mm in dimensions were passed through standard metallographic sample preparation steps up to 1200 mesh emery paper.

RESULTS AND DISCUSSION

The change in hardness values according to the aging time of samples subjected to artificial aging at different durations at 190°C after solutioning treatment for 4 h at 540°C is given in Figure 3.

The commercial hardness value of AA6XXX aluminium alloy was 43 HB, and after solutioning treatment the hardness reduced to 40 HB. As seen in Figure 3, the hardness value of the samples increases with increasing artificial ageing time. The highest hardness value (98 HB) was obtained at 10 h aging time at 190°C. The hardness tended to decrease again with the prolongation of the aging period and the hardness value reduced to 89 HB in 12 h and to 78 HB in 24 h respectively.

Based on the results of the performed investigations, a mathematical relationship between the hardness of the alloy and the heat treatment parameters can be established. Pezda (2014) informed that the mathematical dependence of the effect of heat treatment parameters on the change of the alloy HB hardness is of second order polynomial.

At the end of the aging process, the increase in the hardness values of the alloys is due to variations in the phases, precipitates and grain sizes formed in the microstructure. The increase in hardness is accepted as a sign of the success of the aging process after the dissolution in the literature (Mrowka and Sieniawski, 2005). The highest hardness value can be achieved by adjusting the optimum aging temperature and time.

When the aging process starts, both magnesium and silicon begin to precipitate as Mg_XSi_Y, as indicated by the formula of the solid solution. The precipitate phase formed at the start of aging is in perfect coherence with the aluminium matrix. But at high temperature, the Mg_XSi_Y precipitates become incompatible with the matrix with increasing duration. Because of the artificial aging process, the maximum hardness value of the samples is obtained by precipitation of $β^{II}$ (Mg_5Si_6) phase in needle form. The $β^{II}$ phase begins to turn into a rod like $β^{I}$ (Mg_9Si_5) phase during the increasing aging process, leading to a decrease in the hardness of the material. As the aging time increases, the precipitation of the β (Mg_2Si) phase becomes more dominant, resulting in a marked decrease in the hardness of the aluminium alloy (Li et al., 2013). In this case, full conformity is required to achieve higher strength and stiffness (Pratikno, 2015; El-Menshawy et al., 2012).

At the same time, coarse particles and constantly growing grain sizes are observed due to the combination of increasingly coexisting precipitates in the over aging period. In this period, the factors that prevent dislocation movements keeps decreasing and consequently the mechanical properties of the material are becoming
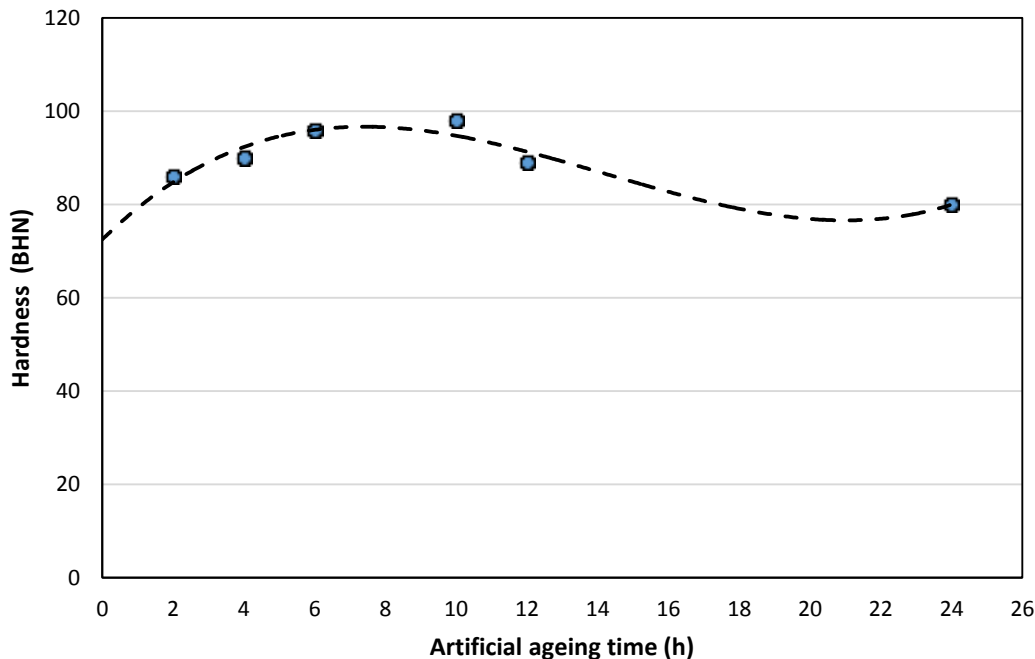
Figure 3. Effect of the artificial aging time on the harness value of AA6XXX alloy.

Table 2. The corrosion test results of AA6XXX samples.

Duration (h)	Ecorr (V)	Icorr ($\mu A/cm^2$)
2	-0.714	15.67
4	-0.838	9.13
6	-0.793	8.49
10	-1.140	1.30
12	-0.721	7.64
24	-0.744	5.73

increasingly smaller (Meyveci et al., 2010).

Corrosion current (Icorr) and corrosion potential (Ecorr) values measured from the corrosion experiments of the samples by the potentiodynamic polarization (Tafel) method are given in Table 2.

The following formulas were used to calculate the corrosion rate (Rcorr) of the samples from these results (Baboian, 2016):

$$R_{corr} = \frac{I_{corr} \cdot K \cdot EA}{d \cdot A}$$

(1)

where:
Rcorr : Corrosion rate (mm/year)
Icorr : Corrosion Current Intensity (μA)
K: Constant (K:3.272×10^{-3} mm/year)
EA: Equivalent weight (atomic weight/valance)
d: Density (g/cm^3)
A: Surface area (cm^2)

The average density of T6 heat treated AA6XXX alloy samples were determined as 2.7013 (g/cm^3) by Archimedes technique. The surface area of samples was 1,1499 cm^2 for corrosion test in this study and K constant was taken as 1.288; also, EA (equivalent weight) was calculated according to the chemical composition of alloy by the formula given below (Baboian, 2016):
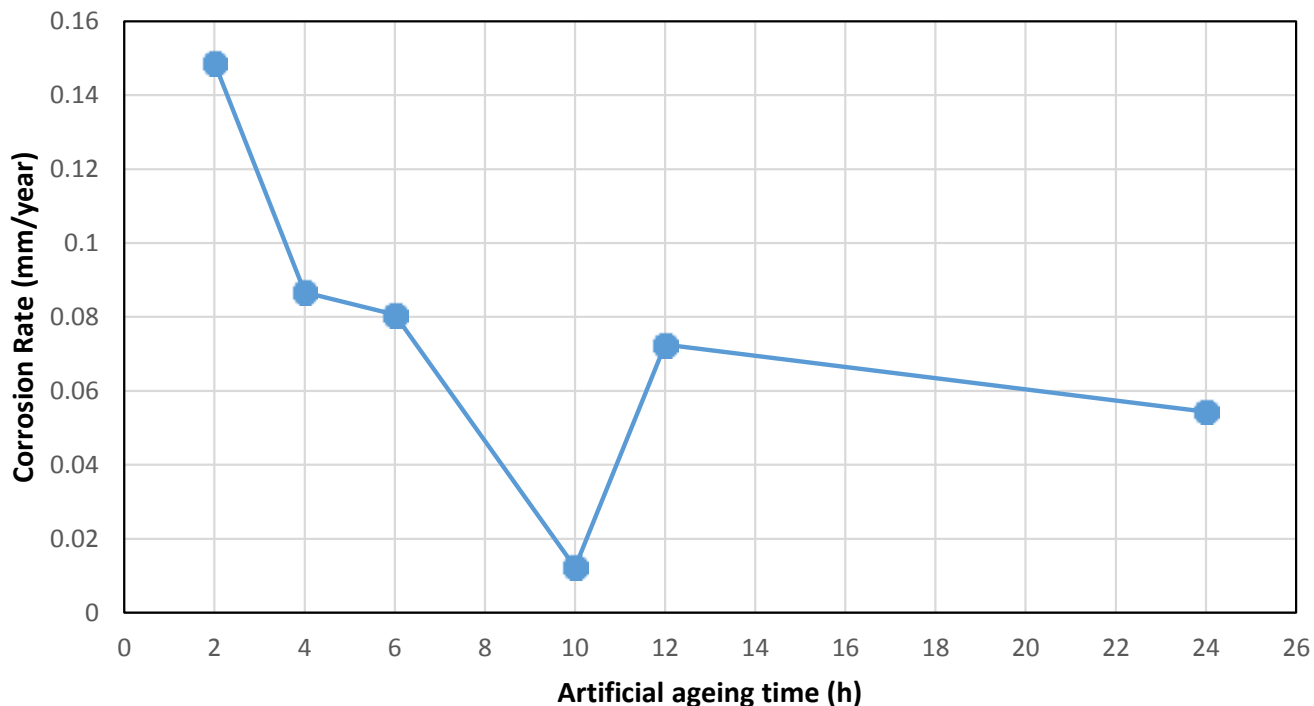
$$EA = \frac{1}{\sum \frac{n.fi}{M_A}}$$

(2)

Where, N: Atomic valance of element
fi: Chemical composition of element
M_A: Atomic weight of element.

When the data of elements of AA6XXX alloy are substituted in the formula, the equivalent weight value is found to be 9.0027. The corrosion rate (Rcorr) was then

Figure 4. The change of corrosion rate with ageing time.

calculated according to the formula given above. The change in corrosion rate with the heat treatment time is plotted in Figure 4.

The corrosion rate of commercial alloy samples was detected as 0.1753 mm/year. As can be seen from Figure 2, the corrosion rate rapidly decreases with aging time and obtained the lowest value of 0.0123 mm/year in 10 h, which is the optimum artificial aging time. In the case of over aging, the corrosion rate increases rapidly and reached 0.0724 mm/year in 12 h.

Aluminium and its alloys are highly resistant to corrosion due to the thin, protective barrier oxide layer on their surface. However, in the presence of chloride ions in the environment this protective oxide layer of the region is likely to suffer from corrosion. The most important factors affecting the corrosion resistance of aluminium alloys are the alloying elements they possess. However, temperatures and durations used in heat treatments also play a dominant role in corrosion behaviour (Jones, 1996).
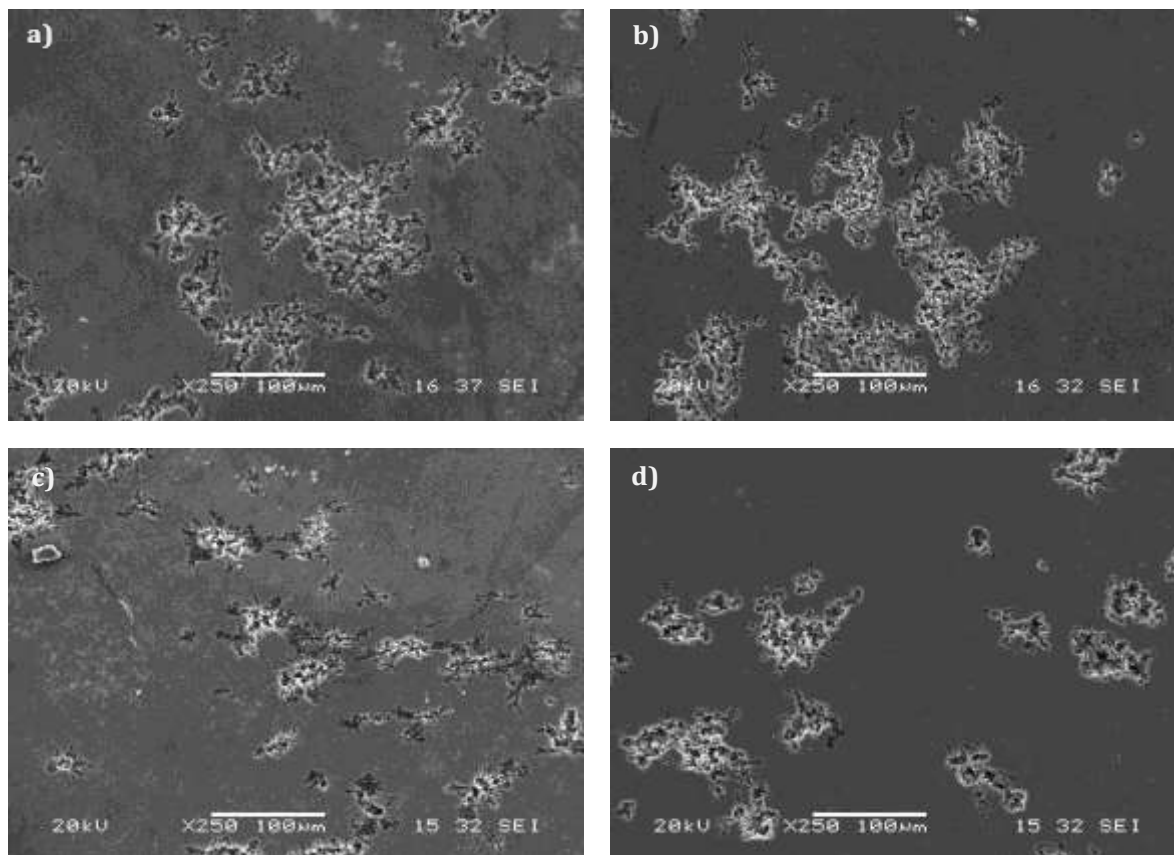
After the corrosion test, surface morphologies of the samples were examined on a SEM microscope. A pronounced pitting corrosion was observed on the surfaces of each specimen (Figure 5). Similar results have been obtained in the literature reviews and it has been observed that with increasing aging period, the pitting corrosion also increases (Svenningsen et al., 2006a). A similar situation has been detected by Yuksel (2017) by the corrosion tests performed to AA6063 alloys artificially aged at different temperatures and durations. It

has been found that intergranular corrosion decreases with increasing aging time, and with the increase of pitting corrosion and over-aging, pitting corrosion becomes dominant.

The corroded areas of the material surface were examined by SEM microscopy and the obtained SEM image and EDS analysis are given in Figure 6 and Table 3, respectively. The EDS analysis of the marked corrosion zone on the microstructure resulted in a concentration of chlorine ions (0.65%) in the corrosive solution, which is similar to many studies in the literature (Yuksel, 2017; Svenningsen et al., 2006a)

When the aging process starts, both Mg and Si are beginning to precipitate in the form of solid solution Mg_2Si and there is an Al matrix around this phase. In this case, electrochemically, the Mg_2Si phase is more active than the Al matrix; so this situation causes the formation of a micro-galvanic corrosion cell and the intergranular corrosion between the phase bound to the grain boundaries and the matrix (Yuksel, 2017).

As the selected temperature for artificial aging process increases, the aging time required to achieve optimum properties is shortened. In this case, however, the increasing aging time leads to the transition of the precipitated phase from needle-shaped to rod-like form (Maisonnette et al., 2011). The increase in pitting corrosion associated with increased aging time is due to the increase in the physical dimension of the more active precipitate phases compared to matrix; although this is not exactly proven (Svenningsen et al., 2006a, b).

Figure 5. The SEM images of corrosion damages variations of AA6XXX alloy according to ageing durations: a) 2 h b) 6 h c)10 h d) 24 h.
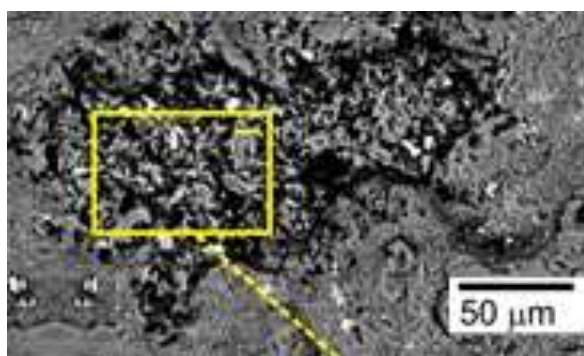
Figure 6. Surface morphology after artificial aging AA6XXX alloy after corrosion test and EDS analysis of corrosion products.

Table 3. EDS analysis of marked area.

Element	Rate (wt.%)
Si	0.62
Mg	0.94
Cl	0.65
Al	98.44

Conclusions

The obtained results from the artificial aging process applied to AA6XXX aluminium alloy at 190°C for 2, 4, 6, 10, 12 and 24 h and their pertinent discussion allow drawing the following conclusions:

1) The AA6XXX Al-Mg-Si alloy exhibits strong ageing response despite having very small amounts of Mg and Si.

2) The experimental results have revealed that aging between 8 and 10 h at 190°C is the most suitable combination of time and temperature imparting maximum corrosion resistance and hardness to the alloy.

3) Up to the completion of the precipitation of the βII phase, a significant increase in the hardness of the material with increasing aging time was obtained and the highest hardness value (98 HB) was detected at the 10-h aging time.

4) With longer aging times, during the transformation of β^{II} phase to β^{I} and β phases (over-aging), the hardness of the alloy decreases rapidly as the sizes and distributions of the precipitates grow out of homogeneity and join with the adjacent precipitates and grow to extreme levels. During 24 h of aging, the hardness value decreased to 78

HB.

5) Likewise, the corrosion rate of alloys is reduced with increasing aging time, and the minimum corrosion rate (0.856 mpy) was obtained at 10-h aging time.

6) In the aging process of the AA6XXX alloy, two types of corrosion were observed, namely intergranular corrosion and pitting corrosion.

7) During the artificial aging, the intergranular corrosion susceptibility of the alloy continues to decrease until the precipitation of the β^{II} phase is complete. However, as the size of the precipitated phase increased, the intergranular corrosion resistance increased, while the susceptibility of the alloy to pitting corrosion increased.

CONFLICT OF INTERESTS

The author has not declared any conflict of interests.

ACKNOWLEDGEMENT

REFERENCES

Baboian R (2016). NACE Corrosion Engineer's Reference Book (4th Edition). NACE International.

Edwards GA, Stiller K, Dunlop GL, Couper MJ (1998). The precipitation sequence in Al–Mg–Si alloys. Acta Materialia 46(11):3893-3904.

El-Menshawy K, El-Sayed AWA, El-Bedawy ME, Ahmed AH, El-Raghy SM (2012). Effect of Aging Time at Low Aging Temperatures on the Corrosion of Aluminum Alloy 6061. Corrosion Science 54:167-173.

Jones DA (1996). Principles and Prevention of Corrosion, Prentice-Hall, Upper Saddle River, NJ.

Li HY, Zeng CT, Han MS, Liu JJ, Lu XC (2013). Time−Temperature−Property Curves for Quench Sensitivity of 6063 Aluminum Alloy, Transactions of Nonferrous Metals Society of China 23(1):38-45.

Maisonnette D, Suery M, Nelias D, Chaudet P, Epicier T (2011). Effect of Heat Treatments on The Microstructure and Mechanical Properties of A 6061 Aluminium Alloy, Materials Science and Engineering A 528:2718-2724.

Mandava S, Ramachandrula S, Yarramareddy A (2014). Effect of Thermal Treatment of a Ferro Magnetic Core on Induced EMF. Procedia Materials Science 6:436-443.

Meyveci A, Karacan I, Caligulu U, Durmus H (2010). Pin-On-Disc Characterization of 2xxx and 6xxx Aluminium Alloys Aged by Precipitation Age Hardening. Journal of Alloys and Compounds 491(1-2):278-283.

Mohamed AMA, Samuel FH (2012). A Review on the Heat Treatment of Al-Si-Cu/Mg Casting Alloys, Heat Treatment - Conventional and Novel Applications, Dr. Frank Czerwinski (Ed.), InTech DOI: 10.5772/50282.

Mrowka GN, Sieniawski J (2005). Influence of Heat Treatment on the Microstructure and Mechanical Properties of 6005 and 6082 Aluminium Alloys, Journal of Materials Processing Technology 162:367-372.

Nandy S, Bakkar MA, Das D (2015). Influence of Ageing on Mechanical Properties of 6063 Al Alloy, Materials Today: Proceedings 2(4-5):1234-1242.

Panigrahi SK, Jayaganthan RA (2010). Study on The Combined Treatment of Cryorolling, Short-Annealing and Aging for The Development of Ultrafine-Grained Al 6063 Alloy with Enhanced Strength and Ductility, Metallurgical And Materials Transactions A 41(10):2675-2690.

Pezda J (2014). The effect of the T6 heat treatment on hardness and microstructure of the EN AC-AlSi12CuNiMg alloy. Metalurgija 53(1):63-66.

Pratikno H (2015). Aging Treatment to Increase the Erosion-Corrosion Resistance of AA6063 Alloys for Marine Application, Procedia Earth and Planetary Science 14:41-46.

Svenningsen G, Larsen MH, Nordlien JH, Nisancioglu K (2006a). Effect of High Temperature Heat Treatment on Intergranular Corrosion of AlMgSi (Cu) Model Alloy, Corrosion Science 48(1):258-272.

Svenningsen G, Larsen MH, Walmsley JC, Nordlien JH, Nisancioglu K (2006b). Effect of Artificial Aging on Intergranular Corrosion of Extruded AlMgSi Alloy with Small Cu Content. Corrosion Science 48(6):1528-1543.

Vargel C (2004). Corrosion of Aluminium, Elsevier. ISBN: 978-0-08-044495-4.

Vissers R, van Huis MV, Jansen J, Zandbergen HW, Marioara CD, Andersen SJ (2007). The crystal structure of the β' phase in Al–Mg–Si alloys. Acta Materialia 55(11):3815-3823.

Wu Y, Liao H (2013). Corrosion Behavior of Extruded near Eutectic Al–Si–Mg and 6063 Alloys. Journal of Materials Science and Technology 29(4):380-386.

Yuksel B (2017). Effect of Artificial Aging on Hardness and Intergranular Corrosion of 6063 Al Alloy, Pamukkale University Journal of Engineering Sciences 23(4):395-398.

Related Journals:

African Journal of
Pure and Applied Chemistry

Journal of
Environmental Chemistry
and Ecotoxicology

Journal of
Geology and Mining Research

Journal of
Internet and
Information Systems

Journal of
Oceanography and
Marine Science

Journal of
Petroleum Technology
and Alternative Fuels

Journal of
Agricultural
Biotechnology and
Sustainable Development

International Journal of
Physical Sciences

Scientific Research and Essays

www.academicjournals.org